

Comparison of three Control Drive Systems for Interior Permanent Magnet Synchronous Motors

M. Caruso, A. O. Di Tommaso, R. Miceli, C. Nevoloso, C. Spataro, F. Viola

Department of Energy, Information Engineering and Mathematical Models, University of Palermo, VialedelleScienze, Building n. 9, 90128 Palermo (Italy), ciro.spataro@unipa.it

Abstract – In a previous paper, we proposed a control strategy for interior permanent synchronous motors, which takes into account also the reduction of the motor power losses. The novelty of the suggested approach is that it takes into consideration the variations of all the motor parameters that have an influence on its efficiency. In order to verify on the field the effectiveness of this new method, we implemented the proposed loss model algorithm in a control drive system and compared its performances, in terms of energy losses with respect to other conventional techniques.

Keywords – interior permanent magnet synchronous motors, power loss minimization, speed control drive systems.

I. INTRODUCTION

Since many years, in the applications that need variable speed and load, the synchronous motors are replacing the DC and the asynchronous motors. A typology of machine that nowadays is more and more used in the low/medium (100 W – 100 kW) industrial and household applications is the synchronous motor with permanent magnets, commonly called brushless motor.

Despite the high cost of the magnets (usually made of samarium-cobalt or neodymium-iron-boron), when these machines are properly driven by the right power converter, they show better performances with respect to the traditional motors, such as:

- higher availability and simpler maintainability;
- higher power density and, therefore, minor weights and volumes;
- higher torque/inertia ratio;
- better dynamic behaviour;
- capability to work to higher values of voltage, speed and torque;
- capability to generate the maximum torque for whatever speed;
- higher efficiency;
- capability to work in inflammable and explosive environments because the lack of slip rings.

Furthermore, these good features continuously

increase thanks to several implementations of new control strategies that allow obtaining the desired values of speed and torque regulating the input quantities (stator voltage and/or currents).

Some of these strategies take into account also the minimization of the power losses by controlling the level of magnetization. However, since the motor efficiency depends on its working conditions (namely speed and load), the losses minimization is not a straightforward task.

The losses reduction approaches can be catalogued in three classes [1-15]: the “simple state control”, the “search control” and the “loss model control”.

The first strategy takes into account only the joule losses trying to reduce them by acting on the displacement between the armature voltages and currents in order to maximize the torque/current ratio or the torque/voltage ratio. However, given that these approaches do not consider the other motor losses, they cannot achieve the minimum losses point.

The second strategy is based on an iterative approach that, by changing step by step a control variable and by monitoring in real time the active power absorbed by the motor, attempts to maximize its efficiency. However, this approach loses its effectiveness, when the motor working conditions vary continuously and rapidly.

The third strategy involves estimating the power losses by means of a mathematical model and regulating a control variable in order to make the motor work at the minimum losses point for whatever speed and/or load. Actually, in order to carry out an accurate estimation, it is necessary to take into account the variation of the motor parameters that influence its efficiency. However, none of the algorithms discussed in literature takes into account simultaneously all the parameter variations of the motor.

For this reason, in a previous paper [16] we presented a detailed characterization of an interior permanent magnet synchronous motor. In particular, the characterization was carried out by assessing, for several working conditions, the aforementioned motor parameters. From the knowledge of the variability of these parameters, we developed a dynamic model of the motor, which accurately describes its behaviour and allows estimating the power losses.

In order to validate both the proposed model and the accuracy on the measurement of the parameters, the values of the power losses obtained by using the model were compared with the values measured with experimental tests.

With the aim to assess the performance of the new “loss model control”, in this paper, we present the comparison of three control strategies. The first one does not take into account the power loss minimization. The second one implements a loss model algorithm, which does not take into account the variability of the motor parameters. The last one implements the new proposed algorithm.

In order to perform this comparison, we decided to subject the motor to two working cycles and to measure the electrical energy absorbed by the motor.

Section II illustrates how the proposed approach was implemented, in section III, the test bench and the measurement setup are described and in section IV, the results of the comparison among the three control algorithms are shown and discussed.

II. IMPLEMENTATION OF THE PROPOSED APPROACH

The “loss model control” strategies are usually based on a well-known motor model (described in detail in [16]) already implemented in several power drive systems. When described in a three-phase coordinate system (a, b, c), the motor model consists of three differential equations with variable coefficients that depend on the angular position of the rotor. Therefore, in order to simplify the mathematical complications, the model is usually converted, by means of the Park transformation, in a two-phase coordinate system (d, q) where the coefficients are independent of the rotor position and, therefore, constant over time. From the transformed model, it is possible to calculate the motor power losses ΔP that are function of:

- the rotor mechanical angular speed ω_m ;
- the direct axis component of the stator phase current i_d ;
- the quadrature axis component of the stator phase current i_q ;
- the direct axis inductance L_d ;
- the quadrature axis inductance L_q ;
- the flux generated by the permanent magnets ψ_{PM} ;
- the resistance of the three-phase stator winding R ;
- the resistance that symbolizes the iron losses R_C .

The last five elements are not adjustable parameters and, for a definite motor working condition (i.e. load and speed), neither ω_m or i_q can be used to control the motor losses. Therefore, the motor efficiency can be controlled only by acting on the i_d value.

The model was developed for the interior permanent magnets synchronous motors (IPMSMs). For these

motors, the presence of the magnets inside the rotor makes the quadrature-axis reluctance lower than the direct-axis reluctance (Fig.1a) and, therefore, L_q is greater than L_d . This difference generates the so-called reluctance torque.

Actually, there are also the surface permanent magnets synchronous motors (SPMSMs). These machines (Fig.1b), from the magnetic viewpoint, can be considered isotropic motor with a large air-gap since the permeability of the magnets is similar to the air permeability. In these cases, $L_q = L_d$ and there is no reluctance torque generation. Therefore, the SPMSM can be studied, as a particular case, by applying the same model of the IPMSM.

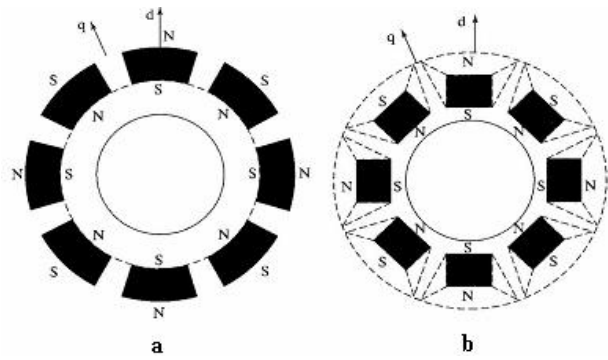


Fig. 1. Transversal sections of a SPMSM (a) e an IPMSM (b)

In any case, to make the model more accurate, it is necessary to consider that these parameters are variable. In particular, the values of the inductances and of the flux of the rotor magnets depend on the magnetic saturation; the armature resistance value depends on its temperature and the iron losses depend on the rotor speed.

In order to verify whether the honed model is able to provide a concrete advantage in the reduction of the power losses, we developed a power drive system, whose block diagram is depicted in Fig. 2.

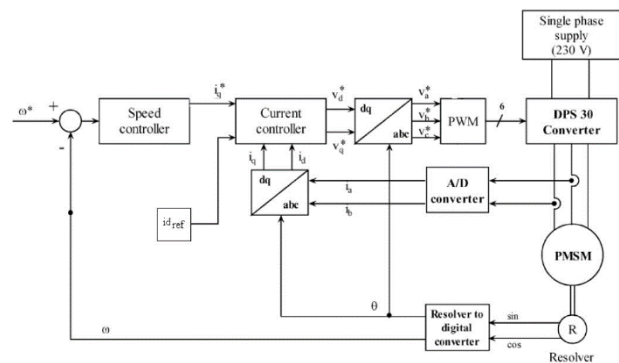


Fig. 2. Block diagram of the power drive system

The used motor (Fig. 3) is a MAGNETIC BLQ-40 three-phase, six-pole brushless machine, with SmComagnets. Table 1 reports its rated values.

Table 1. Rated values of the motor under test

Voltage	132 V
Current	3.6 A
Speed	4000 rpm
Torque	1.8 Nm

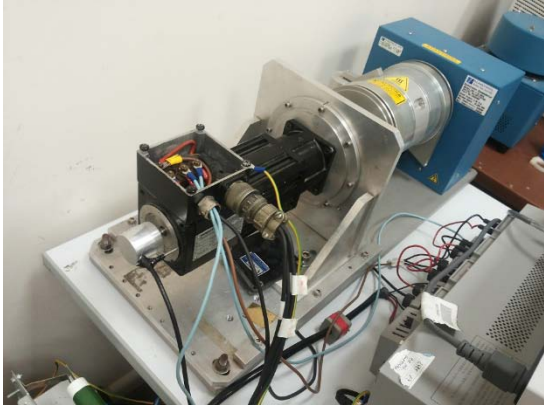


Fig. 3 The IPMSM under test

The motor is supplied by an AUTOMOTION DPS 30 A power converter, directly connected to the electrical grid. The converter is connected to a dSPACE® board that drives the converter IGBT bridge.

This power drive system implements a closed-chain control of the motor speed. The speed reference ω^* is compared with the actual speed ω measured by means of a resolver. The speed error is processed to obtain the reference value of the current quadrature axis component i_q^* .

The system can also act on the magnetization level of the motor, imposing a reference value of the current direct axis component i_d^* . The current references are compared with the actual values of i_q and i_d to get the reference values of the supply voltage Park components v_d^* and v_q^* . These values are reported in a three-phase coordinate system and then, by means of a PWM technique, are applied to the motor.

Depending on how the i_d^* values are chosen, it is possible to change control strategies. In order to evaluate the performances of the proposed approach, we implemented three control algorithms. The first one (ID0) sets $i_d^* = 0$ constantly and, therefore, does not take into account the power losses. The second one (LMA1) applies, as reference, the i_d values obtained by using a loss model algorithm with constant parameters. The last one (LMA2) implements the new proposed algorithm that takes into account the variability of the motor parameters. The used L_d , L_q , ψ_{PM} , R and R_C values are the ones evaluated and reported in [16].

In this case, too, we consider the stator in a thermal steady state. In this way, it is possible to neglect the variability of the armature resistance R , which depends on its temperature.

III. THE MEASUREMENT SETUP

The comparison of the three control algorithms is carried out by subjecting the motor to two working cycles that last for 100 s.

In order to give to the motor the desired torque, we spliced the motor shaft to a MAGTROL HD-715 hysteresis brake (maximum torque 6.2 Nm and maximum speed 30000 rpm). The brake is controlled by a MAGTROL DSP6001 high-speed programmable dynamometer.

As an indicator of the comparison, we evaluated, for the three control algorithms, the cycle energy losses ΔE , calculated as the difference between the active energy E_e absorbed by the converter and the motor shaft mechanical energy E_m . In this way, besides the motor losses, ΔE takes into account the converter losses.

The electrical quantities were assessed by using a YOKOGAWA PZ 4000 three-phase power analyser. The voltage and the current at the converter input were acquired using a frequency rate of 1 kS/s. The voltage and current signals were processed to obtain, every 10 ms, the rms values of voltage and current and the active power absorbed by the converter. Time integrating the active power signal, we obtained the absorbed energy E_e .

In order to assess the mechanical quantities, we acquired, using a frequency rate of 100 S/s, the speed signal, provided by a 26SM19 U452ARTUS resolver, and the torque signal, provided by the aforementioned dynamometer. Multiplying the speed signal by the torque signal, we obtain the mechanical power. Time integrating the power signal, we obtained the energy delivered by the motor E_m .

A discussion about the uncertainty of the energy measurement is deferred to the next chapter.

For each of the two cycles and for each of the three control algorithms, we repeated the test 20 times, using the sequence ID0-LMA1-LMA2. Every six tests, the brake was subjected to a calibration procedure. Altogether, we carried out 120 tests and 20 brake calibrations.

In order to justify the hypothesis of a thermal steady state and to guarantee an approximately constant stator winding temperature, all the measurements were carried out in the following way. After every brake calibration, we let the motor work at the full speed and load until its external temperature reached the thermal equilibrium (67.0 °C). Then, we carried out a series of six tests.

IV. RESULTS

In order to test the performances of the three control algorithms, we selected two working cycles that are representative of industrial applications.

The cycle I (whose speed and torque profile is reported in Fig. 4) is characterized by constant speed and variable torque. The cycle II (whose speed and torque

profile is reported in Fig. 5) is characterized by constant torque and variable speed.

As an example for the cycle I, Figs. 6-9 show the time trends of the rms voltage, the rms current, the active power and the active energy acquired during one of the 20 tests. These graphs, for the sake of clarity, show only the comparison between ID0 e LMA2, whereas the LMA1 data is omitted.

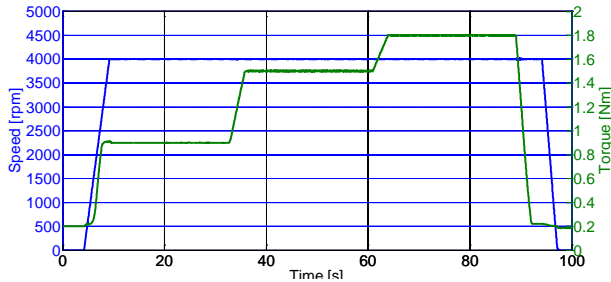


Fig. 4. Speed and torque profiles for cycle I

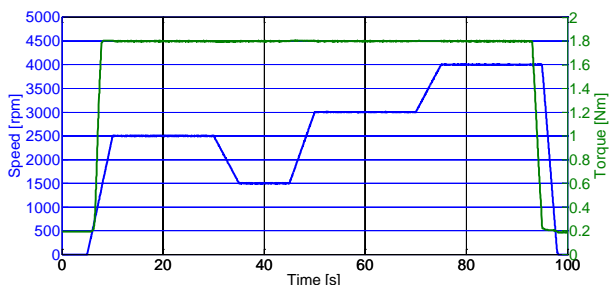


Fig. 5. Speed and torque profiles for cycle II

Table 2 reports, for the three control algorithms, both the mean values and the standard deviations of:

- the active energy absorbed by the converter that is the input energy (E_m);
- the mechanical energy provided at the motor shaft that is the output energy (E_e);
- the energy losses (ΔE);
- the system efficiency (η);
- the saved energy (E_s) calculated as difference of the actual losses ΔE and the mean value of the losses measured when ID0 is implemented.

It is possible to notice that, on average, the usage of LMA1 entails a 663 J reduction of the energy losses and a 1.1 % efficiency increase, compared to the ID0 performances. The usage of LMA2, in turn, entails a 161 J reduction of the energy losses and a 0.3 % efficiency increase, compared to the LMA1 performances.

Similar results were obtained for cycle II (Figg. 10-13 and Table 3). In this case, on average, the usage of LMA1 entails a 568 J reduction of the energy losses and a 1.0 % efficiency increase, compared to the ID0 performances. The usage of LMA2, in turn, entails a 176 J reduction of the energy losses and a 0.3 % efficiency increase, compared to the LMA1 performances.

Analysing the obtained data, it could seem that taking into account the variability of the motor parameters

provide just a modest advantage in the reduction of the power losses. It is worthwhile to underscore, however, that the LMA1 performances depends on how well the chosen values of the motor parameters (mean values, rated values, maximum values or modal values) comply with the actual motor average speed and average load. On the contrary, LMA1 is able to find the minimum losses point for whatever speed and load. Therefore, for working cycles, which alternate no-load/full-load sequences or stop/full-speed sequences, the differences between the LMA1 and LMA2 performances are expected to be higher.

Moreover, the study of the equations of the motor model demonstrates that the differences between the LMA1 and LMA2 performances are more significant for the motors with high value of the reluctance torque.

The last considerations show that the usage of a loss model algorithms, which take into account the variability of the parameters, can be, in any case, recommended.

The uncertainty evaluation of the energy measurements was carried out starting from the analysis of the measurement repeatability, which is represented by the standard deviation. From Table 2 and Table 3, it is possible to notice that, both for the input energy and the output energy, the standard deviation is quite high (500 – 600 J). This limited repeatability is generated by the torque oscillations due to the operating principle of the hysteresis brake. Nevertheless, given that when the torque increase, the converter current tends to increase too, there is a high correlation between the measures of E_e and E_m . This entails a reduction of the standard deviation of their difference (the energy losses) and of their ratio (the efficiency).

Obviously, the repeatability takes into account only the effect of the random errors and, therefore, it is necessary to consider the systematic components of uncertainty too. Let us neglect the random errors. If there were only the systematic errors, indicating with $u(E_e)$ the uncertainty on the E_e measurement and with $u(E_m)$ the uncertainty on the E_m measurement, the uncertainty of their difference is

$$u(\Delta E) = u(E_e - E_m) = \sqrt{u^2(E_e) + u^2(E_m)}$$

Similarly, indicating with $\hat{u}(E_e)$ the relative uncertainty on the E_e measurement and with $\hat{u}(E_m)$ the relative uncertainty on the E_m measurement, the uncertainty of their ratio is

$$\hat{u}(\eta) = \hat{u}\left(\frac{E_m}{E_e}\right) = \sqrt{\hat{u}^2(E_m) + \hat{u}^2(E_e)}$$

As for the saved energy (difference of the actual losses ΔE and the mean value of the losses ΔE_{ID0} measured when ID0 is implemented), considering that $u(E_e) = u(E_{eID0})$ and $u(E_m) = u(E_{mID0})$, the uncertainty is

$$u(E_s) = u(\Delta E - \Delta E_{ID0}) = u(E_e - E_m - E_{eID0} + E_{mID0}) = \sqrt{2u^2(E_e) + 2u^2(E_e) - 2u^2(E_e) - 2u^2(E_m)} = 0$$

It is possible to notice that the systematic errors increase in the measurement of ΔE and η , but cancel in the measurement of E_s , which is the most significant indicator of the comparison among the three algorithms. Therefore, the repeatability of the E_s measurement can be considered an accurate estimate of the standard uncertainty $u(E_s)$.

Table 2. Measured data for cycle I

		Input Energy [J]	Output Energy [J]	Energy Losses [J]	Efficiency [%]	Saved Energy [J]
ID0	Mean	53774	46422	7352	86.3	0
	St.Dev.	577	591	86	0.2	86
LMA1	Mean	53089	46400	6689	87.4	663
	St.Dev.	622	643	95	0.2	95
LMA2	Mean	52924	46396	6528	87.7	824
	St.Dev.	555	582	80	0.2	80

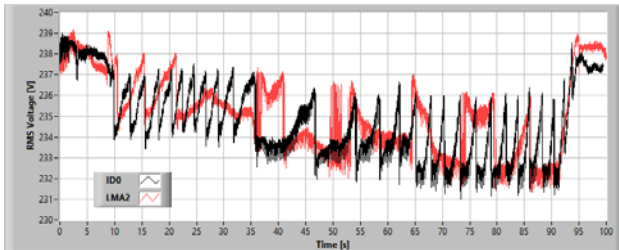


Fig. 6. Rms voltage for cycle I

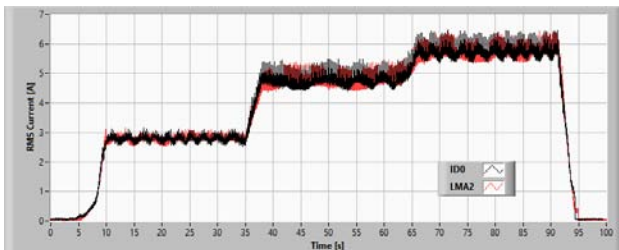


Fig. 7. Rms current for cycle I

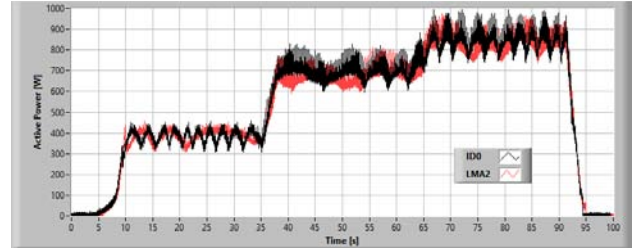


Fig. 8. Active power for cycle I

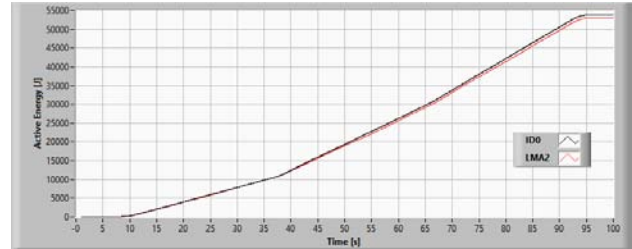


Fig. 9. Active energy for cycle I

Table 3. Measured data for cycle II

		Input Energy [J]	Output Energy [J]	Energy Losses [J]	Efficiency [%]	Saved Energy [J]
ID0	Mean	54350	47472	6878	87.3	0
	St.Dev.	587	540	81	0.2	81
LMA1	Mean	53800	47492	6309	88.3	568
	St.Dev.	501	599	90	0.2	90
LMA2	Mean	53616	47484	6132	88.6	744
	St.Dev.	488	524	66	0.2	66

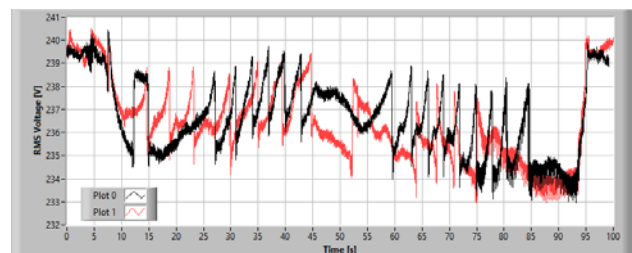


Fig. 10. Rms voltage for cycle II

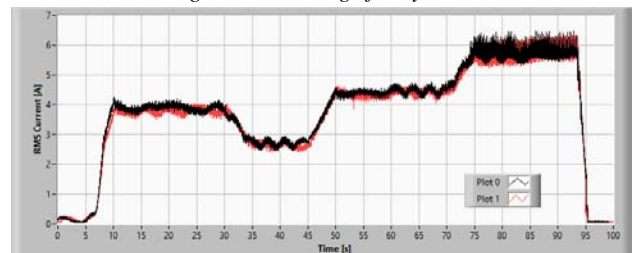


Fig. 11. Rms current for cycle II

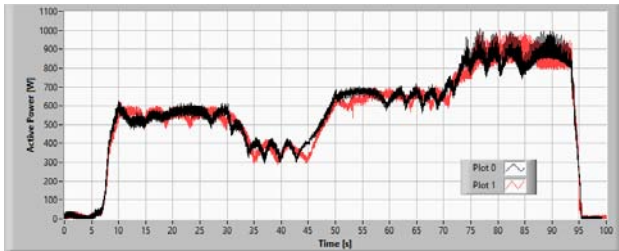


Fig. 12. Active power for cycle II

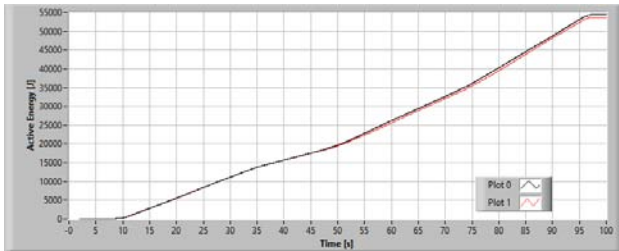


Fig. 13. Active energy for cycle II

V. CONCLUSIONS

In the paper, we described the development of a power drive system that implements a loss model algorithm. The system can drive a low power interior permanent magnets synchronous motor and, besides controlling speed and torque of the motor, is able to reduce its power losses.

The novelty of the system is that the loss model algorithm takes into account the variability of all the parameters that have an impact on the motor efficiency.

In order to verify if the proposed system is able to provide a concrete advantage, we compared its performances in terms of energy losses with the performance of classic power drive systems.

The experimental results shown that the usage of a variable parameters loss model algorithm leads to an evident, (though modest for the particular tested motor), increase of the motor efficiency.

The next step of our work will be the characterization of a medium power (10 kW) IPMSM with a significant reluctance torque and the design of its power drive system.

For this motor, the difference between LMA1 and LMA2 performances are expected to be more substantial.

VI. ACKNOWLEDGMENT

This work was financially supported by MIUR - Ministero dell'Istruzione, dell'Università e della Ricerca (Italian Ministry of Education, University and Research) and by SDESLab (Sustainable Development and Energy Saving Laboratory) of the University of Palermo.

REFERENCES

[1] C. Mademlis, J. Xypteras, and N. Margaris, *Loss minimization in surface permanent-magnet synchronous motor drives*,

Industrial Electronics, IEEE Transactions on, vol. 47, pp. 115–122, Feb 2000.

[2] A. Bazzi and P. Krein, *Review of methods for real-time loss minimization in induction machines*, *Industry Applications, IEEE Transactions on*, vol. 46, pp. 2319–2328, Nov 2010.

[3] C. Mademlis, I. Kioskeridis and N. Margaris, *Optimal efficiency control strategy for interior permanent-magnet synchronous motor drives*, in *IEEE Transactions on Energy Conversion*, vol. 19, no. 4, pp. 715-723, Dec. 2004.

[4] S. Vaez, V. I. John and M. A. Rahman, *An on-line loss minimization controller for interior permanent magnet motor drives*, in *IEEE Transactions on Energy Conversion*, vol. 14, no. 4, pp. 1435-1440, Dec 1999.

[5] C. Mademlis, J. Xypteras and N. Margaris, *Loss minimization in surface permanent-magnet synchronous motor drives*, in *IEEE Transactions on Industrial Electronics*, vol. 47, no. 1, pp. 115-122, Feb 2000.

[6] C. Cavallaro, A. O. Di Tommaso, R. Miceli, A. Raciti, G. R. Galluzzo and M. Trapanese, *Efficiency Enhancement of Permanent-Magnet Synchronous Motor Drives by Online Loss Minimization Approaches*, in *IEEE Transactions on Industrial Electronics*, vol. 52, no. 4, pp. 1153-1160, Aug. 2005.

[7] J. Lee, K. Nam, S. Choi e S. Kwon, *A Lookup Table Based Loss Minimizing Control for FCEV Permanent Magnet Synchronous Motors*, *Proc. of IEEE Vehicle Power and Propulsion Conference*, Arlington, TX, pp. 175-179, 2007.

[8] C. Mademlis and N. Margaris, *Loss minimization in vector-controlled interior permanent-magnet synchronous motor drives*, in *IEEE Transactions on Industrial Electronics*, vol. 49, no. 6, pp. 1344-1347, Dec 2002.

[9] C. Mademlis e V. G. Agelidis, *On Considering Magnetic Saturation with Maximum Torque to Current Control in Interior Permanent Magnet Synchronous Motor Drives*, *IEEE Transactions on energy conversion*, vol. 16, no. 3, September 2001.

[10] J. Lee, K. Nam e S. Choi, *Loss-Minimizing Control of PMSM With the Use of Polynomial Approximations*, *IEEE Transactions on power electronics*, vol. 24, no. 4, April 2009.

[11] S. Morimoto, Y. Tong e Y. Takeda, *Loss Minimization Control of Permanent Magnet Synchronous Motor Drives*, *IEEE Transactions on industrial electronics*, vol. 41, no. 5, October 1994.

[12] M. Fazil and K. R. Rajagopal, *Nonlinear dynamic modeling of a singlephase permanent-magnet brushless DC motor using 2-d static finiteelement results*, *Magnetics, IEEE Transactions on*, vol. 47, pp. 781–786, April 2011.

[13] O. Mohammed, S. Liu, and Z. Liu, *A phase variable model of brushless dc motors based on finite element analysis and its coupling with external circuits*, *Magnetics, IEEE Transactions on*, vol. 41, pp. 1576–1579, May 2005.

[14] A. Matsumoto, M. Hasegawa, and S. Doki, *A novel IPMSM model for robust position sensorless control to magnetic saturation*, *Proc. of Power Electronics Conference (IPEC-Hiroshima 2014 - ECCE-ASIA)*, 2014 International, pp. 2445–2450, May 2014.

[15] Z. Li and H. Li, *MTPA control of PMSM system considering saturation and cross-coupling*, *Proc. of Electrical Machines and Systems (ICEMS)*, 2012 15th International Conference on, Sapporo, 2012, pp. 1-5.

[16] M. Caruso, A. O. Di Tommaso, R. Miceli, C. Nevoloso, C. Spataro, F. Viola, *Characterization of the parameters of interior permanent magnet synchronous motors for a loss model algorithm*, in *Measurement, Volume 106*, August 2017, Pages 196–202.